Reaction Mechanism of the Selective Catalytic Reduction of NO with NH_3 and O_2 to N_2 and H_2O†

Karl Jug,* Thorsten Homann, and Thomas Bredow

Theoretische Chemie, Universität Hannover, Am Kleinen Felde 30, 30167 Hannover, Germany

Received: September 30, 2003; In Final Form: November 24, 2003

Semiempirical MSINDO calculations were performed to study the selective catalytic reduction of NO to N_2 on vanadium pentoxide supported by anatase. The active part of the surface was modeled by V_2O_7 species bound to the anatase (100) surface, which in turn was modeled by a sufficiently large anatase cluster saturated by H and OH groups at the periphery. The whole reaction mechanism consisted of 24 steps and involved NH_3, NO and O_2 at the reactant side and N_2 and H_2O on the product side. All intermediates and transition structures were optimized under partial relaxation of the surface. The energy profile along the reaction pathway was calculated and it could be shown that the reaction is feasible.

1. Introduction

The present environmental problems are caused mainly by the emission of pollutants. Among them, the nitrogen oxides NO_x produced by fuel combustion are most prominent.[1−3] NO_x is a mixture of about 95% NO and 5% NO_2. It is therefore of utmost importance to design processes for the removal of NO from the atmosphere. For stationary sources this can be achieved by selective catalytic reduction (SCR)[4] of NO by NH_3. Despite its widespread technological use, the reaction mechanism of the NO reduction is not fully understood. Busca et al.[5] reviewed the chemical and mechanistic aspects of the SCR of NO_x by ammonia over oxide catalysts. The authors have collected experimental data and mechanistic models presented in the literature. The most important catalysts are based on vanadium pentoxide. The TiO_2 anatase serves as support. The questions that are raised concern the adsorption characteristics of NH_3 and NO over such oxide-based catalysts. Several models for the bonding of NH_3 to the catalytic surface are discussed which comprise Lewis-bonded NH_3 at titanium sites, hydrogen-bonded NH_3 on oxygen sites, Lewis-bonded NH_3 at vanadyl sites and ammonia adsorbed as ammonium ions over Brønsted acidic OH surface hydroxy groups. When it was concluded that NO, not NO_2, is the actual reactant in the SCR[6] and that oxygen participates in the reaction,[7,8] the following stoichiometric equations could account for the reaction process

$$4NH_3 + 4NO + O_2 \rightarrow 4N_2 + 6H_2O \qquad (1)$$

This is supported by experiments with isotopically labeled reactants from which it was concluded that for vanadia-based catalysts the two nitrogen atoms of N_2 arise, one from NO and the other from NH_3.[9,10] It is also agreed that under typical SCR conditions with consumption of equal amounts of NH_3 and NO only a small amount of oxygen is involved. This means that the reaction

$$4NH_3 + 4NO + 3O_2 \rightarrow 4N_2O + 6H_2O \qquad (2)$$

is not significant. To avoid unselective behavior with unwanted byproducts, it is therefore important to provide equal amounts of NH_3 and NO in the experimental setup.

A few theoretical studies for the reaction of NH_3 with NO on V_2O_5 cluster models[11−13] have appeared or are to appear.[14] In these studies the surface was modeled by small clusters and the active sites for adsorption were investigated. No full reaction mechanism was presented. The goal of our work is therefore to derive a full sequence of reaction steps including intermediates and transition structures to elucidate the reaction mechanism of eq 1.

2. Modeling

Modeling of the surface of the vanadia−titania catalyst is a crucial part. It should be in line with experimental information. Such combined catalysts can be prepared by milling[15] or by impregnation.[16] In the first case an oxide mixture is prepared in a planetary mill; in the second case TiO_2-anatase is impregnated by solutions of vanadyl oxalate or ammonium vanadate. In both cases V_2O_5 particles appear on the surface. The amount of V_2O_5 is much smaller than that of TiO_2. High catalytic activity was found for a coverage of a monolayer or less. To characterize the surface, the local environment of vanadium centers can be studied with solid state ^{51}V NMR. Two types of V^{5+} species were found to be strongly bound to the TiO_2 surface. They deviate from the axial symmetry of V_2O_5. Besides three types of V^{4+} species were found which are separated from the V^{5+} centers. Deo and Wachs[17,18] studied different VO_x coverages of anatase with Raman and ^{51}V NMR spectroscopy. For low coverages of 1% they found metavanadates $(VO_3)_n$ and decavanadates $(V_{10}O_{28})^{6-}$. With increasing coverage the decavanadate portion was increasing and was dominant for a monolayer. Other authors[5] found also monomeric VO_4 and dimeric V_2O_7 species on the anatase surface. Forzatti[19] reported monomeric VO_4 for low coverage and polymeric metavanadate species for higher coverage, but did not quantify the coverage. Bulushev et al.[20] have used a variety of methods to arrive at the conclusion that both VO_4 species and polymeric metavanadate species coexist on the anatase surface at low coverage. The same observation was made by Lietti and Forzatti[21] for a submonolayer coverage. By ^{51}V NMR studies Pinaeva et al.[22] found at low coverages two kinds of V atoms

† Part of the special issue "Fritz Schaefer Festschrift".

10.1021/jp031113i CCC: $27.50
Published on Web 01/22/2004

which were bound to O atoms in distorted tetrahedral arrangements. These authors find octahedral arrangement only for high coverage. Secondary ion mass spectrometry (SIMS) experiments on VO_x/TiO_2 catalysts identified $V_xO_yH^+$ and V_2O_x ions,[23] which suggest vanadate chains[24] on the anatase surface. From these and other experimental studies[25−28] it appears that the VO_x species on the anatase surface have low coordination and are isolated and that the existence of polymeric vanadate is very likely.[29] Such models were already reviewed a few years ago.[5]

Theoretical models for combined V_2O_5/TiO_2 catalysts are rare. The simplest type of modeling is by semiclassical potentials.[30] Here various V_2O_5/TiO_2 interfaces were modeled. It was concluded that significant structural differences exist between the surface of a supported V_2O_5 monolayer on the TiO_2 anatase compared with the unsupported V_2O_5 surface with implications for the catalytic behavior of such material. A rather artificial model is presented by Anstrom et al.[13] where very small saturated V_2O_5 and TiO_2 clusters are placed adjacent to each other without any bonding between these clusters, rather an NH_3-NHO unit is placed between and considered as adsorbed. Calatayud et al.[31] proposed dimeric and cyclic vanadyl species with V_2O_5 stoichiometry which were placed on (100) and (001) surfaces and which were investigated by a periodic method. Alternatively, Ti atoms were replaced by V atoms on the anatase (110) and (001) surfaces.[32] Whereas these investigations were periodic DFT studies, other work by some of these authors[33] was on small cluster models. We have found that the substitution model is less supported in terms of experimental evidence and we have therefore pursued a model consisting of a dimeric V_2O_7 species placed on an anatase (100) surface that is modeled by clusters of medium and large size. Due to its structure this surface is particularly suited as support for isolated VO_4 species or polyvanadate-like chains which are assumed to be the reactive species in the SCR process.[5] This is in line with the experimental results of Bulushev et al.[20] The smaller cluster was $V_2O_7H_4Ti_{33}O_{66}(H_2O)_{17}$, the larger $V_2O_7H_4Ti_{132}O_{264}(H_2O)_{48}$. The four hydrogen atoms are assumed to be produced in the ammonium vanadate impregnation process. One possibility is realized in the following reaction under the assumption of dissociative water adsorption on the anatase surface as an introductory step in solution

$$2(NH_4)_3VO_4 + 4Ti(OH)_2 \rightarrow 6NH_3 + V_2O_7(TiOH)_4 + 5H_2O \quad (3)$$

The dissociative adsorption of H_2O on the anatase (100) surface was found to be more stable than the molecular adsorption by 37 kJ/mol. The water molecules and hydrogen atoms serve to restore the proper saturation of the cluster at the periphery by H and OH groups and to retain stoichiometry $(V_2O_5)_l(TiO_2)_m(H_2O)_n$. H saturates the oxygen and OH the titanium for those atoms of anatase which are not surface atoms.

3. Reaction Mechanism

Our initial work on transition metal oxides included studies of OH radical formation on anatase particles[34] and H adsorption on vanadium pentoxide.[35] The calculations were on medium size free or saturated clusters. The underlying method was SINDO1, which was parametrized for first-row[36] and for third-row transition metal[37] elements. In the meantime the parametrization for first-row elements was much improved[38,39] for structures and heats of formation and a similar improvement was achieved for first-row transition metal elements[40] in the newly developed MSINDO method. We therefore started our investigation on the reaction mechanism with a study of adsorption of H, NH_3, H_2O, and NO on the (001) surface of vanadium pentoxide.[41] The V_2O_5 was again modeled by saturated V_2O_5 clusters of $(V_2O_5)_n(H_2O)_m$ type ($n = 24-54$, $m = 20-40$). Strong adsorption was found for H, NH_3, and H_2O, but we found no adsorption for NO. Similar adsorption studies were completed for TiO_2 anatase[42] and V_2O_5/TiO_2.[43] The relaxation scheme for surface atoms of the two cluster models is depicted in Figure 1. The relaxation includes the V_2O_7 unit, which is the adsorption site, as well as those Ti atoms, which are connected to the V atoms via O atoms, their next neighbors on anatase, and the four H atoms. Table 1 presents the adsorption energies of NH_3, NO, and H_2O on the two clusters $V_2O_7H_4Ti_{33}O_{66}(H_2O)_{17}$ and $V_2O_7H_4Ti_{132}O_{264}(H_2O)_{48}$ under the described relaxation scheme together with the corresponding experimental data.[44−47] It can be seen that the adsorption energies are almost converged with the smallest cluster model and that there is good agreement with experimental data. Therefore the $V_2O_7H_4Ti_{33}O_{66}(H_2O)_{17}$ cluster (Figure 2) was chosen for the study of the reaction mechanism, because the calculation is much less time-consuming.

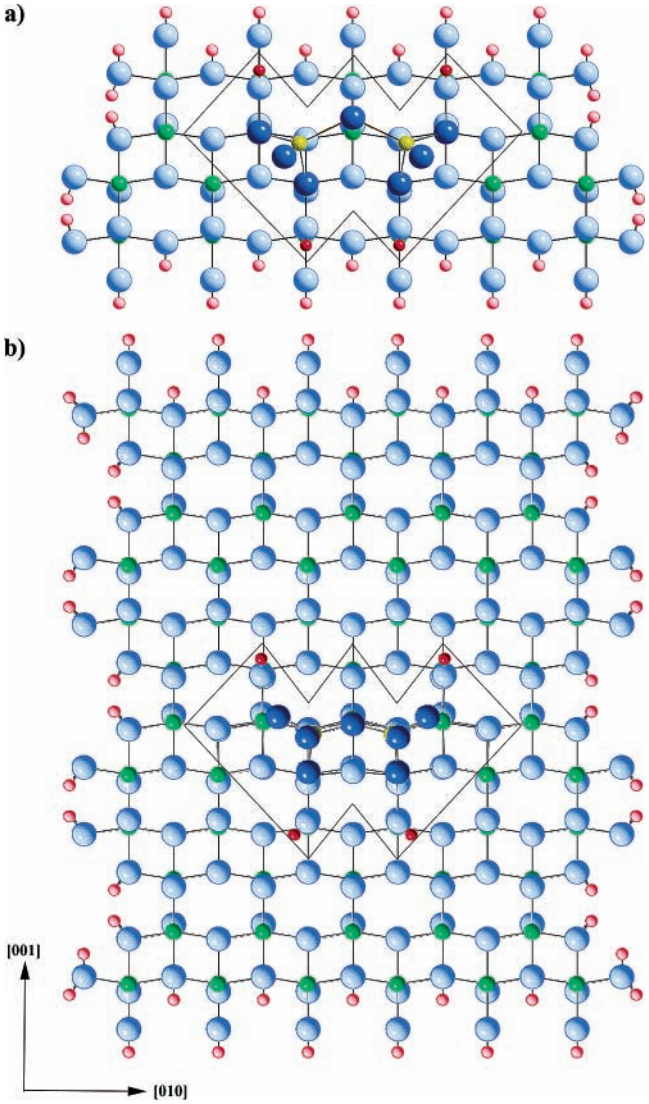

Figure 1. Relaxation region on the surface of the (a) $V_2O_7H_4Ti_{33}O_{66}(H_2O)_{17}$ and (b) $V_2O_7H_4Ti_{132}O_{264}(H_2O)_{48}$ clusters: V (yellow); O (dark blue); H (dark red); Ti (green); O (light blue); H (light red); O (light blue).

Two types of mechanisms play a role in heterogeneous catalysis: the Langmuir−Hinshelwood mechanism, according

TABLE 1: Adsorption Energies (kJ/mol) for Molecules NO, NH_3, and H_2O on $V_2O_7H_4Ti_{33}O_{66}(H_2O)_{17}$ and $V_2O_7H_4Ti_{132}O_{264}(H_2O)_{48}$

	adsorption energies (kJ mol^{-1})		
cluster	NO	NH_3	H_2O
$V_2O_7H_4Ti_{33}O_{66}(H_2O)_{17}$	−36	−128	−58
$V_2O_7H_4Ti_{132}O_{264}(H_2O)_{48}$	−28	−117	−48
		−100 to −130[a]	
		−92 to −117[b]	
exp	−20[a]		−59 to −75[c]
		−75 to −109[c]	
		−75 to −109[d]	

[a] Reference 44. [b] Reference 45. [c] Reference 46. [d] Reference 47.

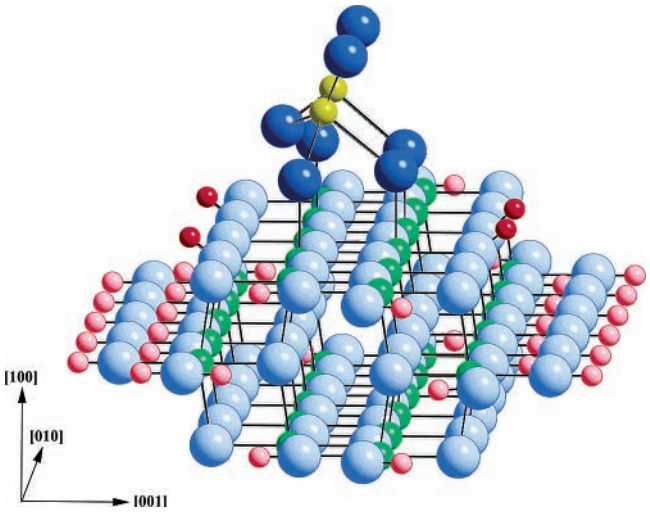

Figure 2. Side view of $V_2O_7H_4Ti_{33}O_{66}(H_2O)_{17}$.

to which the reactants are adsorbed from the gas or liquid phase on the surface of the catalyst and react there to the product, or the Eley−Rideal mechanism, where it is assumed that one reactant is adsorbed and the second reactant reacts from the gas or liquid phase with the adsorbed reactant. The majority of experimentalists[4,19,48−50] conclude from the observed rate law for NO participation that NO reacts from the gas phase whereas NH_3 is adsorbed. We have therefore chosen the Eley−Rideal mechanism as a basis for our studies.

We have subdivided the reaction scheme in two parts. Figure 3 shows the first part of the reaction scheme from the reactant **R** with the approach of an NH_3 molecule to the vanadium of a vanadyl group until the involvement of the oxygen molecule. This presents about half of the reaction scheme. The other part is illustrated in Figure 4 and shows the reaction from the intermediate with the hydroxoperoxy group to the final product P. In the following, energies E_{rel} relative to the reactants according to eq 1 are presented. We first discuss the intermediates I and their energies E_{rel}(I), which are listed in Table 2. The structures were optimized with a Broyden−Fletcher−Goldfarb−Shanno (BFGS) method. A part of the surface atoms were relaxed according to the procedure described above.

The reaction starts with the adsorption of an NH_3 molecule at a V atom as Lewis acid center (**1**) as proposed by Ramis et al.[51] In this step an energy of $E_{rel} = -128$ kJ/mol is released. Thereafter the active catalyst center is rearranged in such a way that an isolated VO_4 unit arises and the adsorption site is surrounded by three oxygen atoms and the adsorbed NH_3 in a tetrahedral arrangement (**2**). This leads to another lowering of the energy to −172 kJ/mol. From coordination chemistry it is known that the ions of vanadium in their high oxidation states prefer tetrahedral arrangement of their ligands,[52] which explains

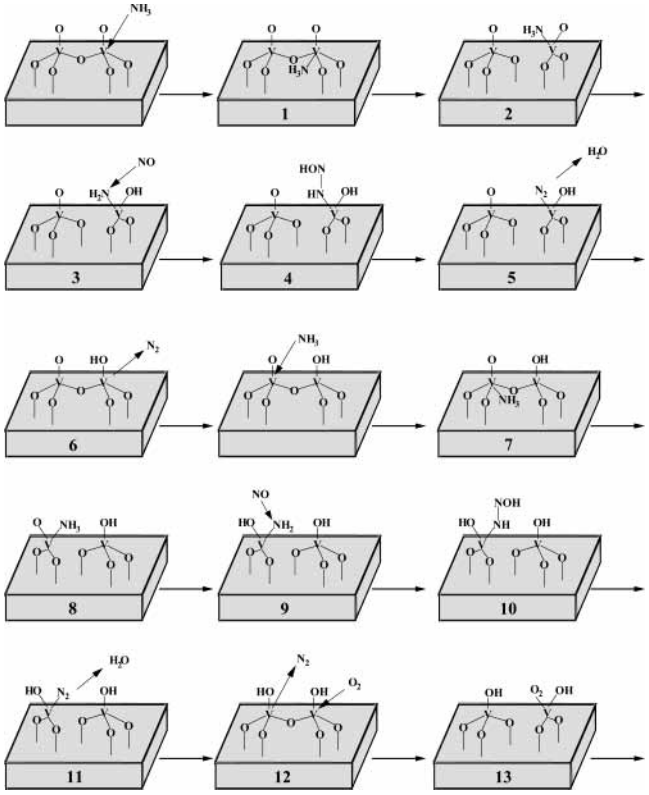

Figure 3. Reaction scheme from reactants **R** to intermediate **13** with O_2 involvement.

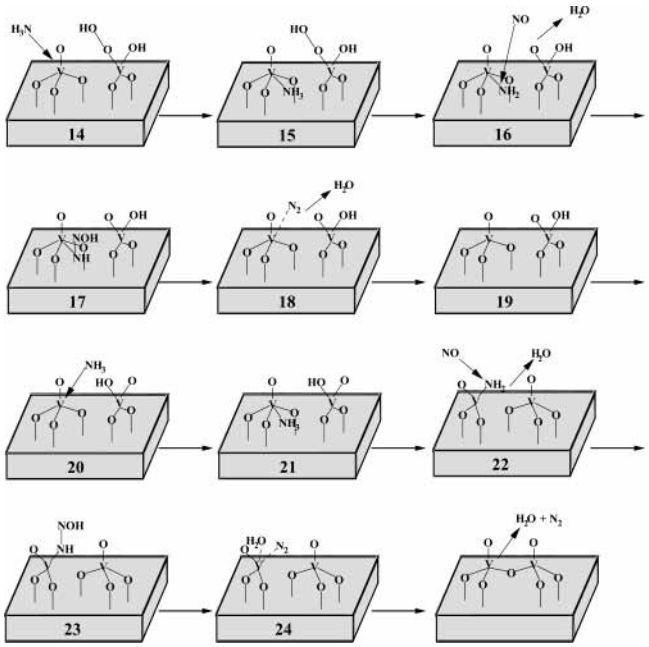

Figure 4. Reaction scheme from intermediate **14** with hydroxoperoxy group to products **P**.

step **2**. The N atom of the adsorbed ammonia has a reduced electron density compared to the free NH_3 molecule. This means that its Brønsted acidity is increased. In this way transfer of a hydrogen atom to the neighboring vanadyl oxygen is facilitated. This does not change the oxidation number of vanadium. The relative energy of the corresponding intermediate (**3**) is −126 kJ/mol. Such an intermediate is supported by Fourier transform infrared (FTIR) spectra, which indicate the existence of NH_2 species.[5] In the next step an intermediate (**4**) is generated by the reaction of the V−NH_2 group with an NO molecule from

TABLE 2: Relative Energies E_{rel}(I) (kJ mol^{-1}) of the Reaction Intermediates I

I	M^b	reaction	mechanistic step	E_{rel}(**I**)
R[a]	1			0
1	1	$VO_3-O-VO_3NH_3$	NH_3 adsorption	−128
2	1	$VO_4 + VO_3NH_3$	NH_3 activation	−172
3	1	$VO_4 + HOVO_2NH_2$	H transfer from NH_3 to V═O	−126
4	2	$VO_4 + HOVO_2NH-NOH$	formation of nitrosamine species	−217
5	2	$VO_4 + HOVO_2N_2 + H_2O$	desorption of H_2O	−383
6	2	$HOVO_2-O-VO_3 + N_2$	desorption of N_2	−295
7	2	$HOVO_2-O-VO_3 + NH_3$	NH_3 adsorption	−417
8	2	$HOVO_3 + VO_3NH_3$	NH_3 activation	−450
9	2	$HOVO_3 + HOVO_2NH_2$	H transfer from NH_3 to V═O	−428
10	3	$HOVO_3 + HOVO_2NH-NOH$	formation of nitrosamine species	−500
11	3	$HOVO_3 + HOVO_2N_2 + H_2O$	desorption of H_2O	−732
12	3	$HOVO_2-O-VO_2OH + N_2$	desorption of N_2	−595
13	1	$HOVO_3 + HOVO_2O_2$	adsorption of O_2	−1107
14	1	$VO_4 + HOOVO_2OH$	H abstraction from adjacent $HOVO_3$ group	−1029
15	1	$H_3NVO_4 + HOOVO_2OH$	NH_3 adsorption	−1118
16	1	$H_2NVO_4 + OVO_2OH + H_2O$	H abstraction from adsorbed NH_3	−1177
17	2	$HONNHVO_4 + OVO_2OH$	formation of nitrosamine species	−1144
18	2	$N_2VO_4 + H_2O + OVO_2OH$	desorption of H_2O	−1316
19	2	$VO_4 + OVO_2OH + N_2$	desorption of N_2	−1283
20	2	$VO_4 + HOVO_2O$	H transfer	−1283
21	2	$H_3NVO_4 + HOVO_2O$	NH_3 adsorption	−1360
22	2	$H_2NVO_2O + VO_4 + H_2O$	H abstraction from adsorbed NH_3	−1275
23	1	$HONNHVO_2O + VO_4$	formation of nitrosamine species	−1589
24	1	$H_2ON_2VO_2O + VO_4$	decomposition of nitrosamine species	−1745
P[a]	1	$VO_3-O-VO_3 + H_2O + N_2$	desorption of H_2O and N_2	−1655

[a] R: reactants. P: products. [b] *M*: multiplicity.

the gas phase. This corresponds to the experimental results of Ramis et al.[51] The intermediate V−NH−NOH corresponds to the tautomerized nitrosamine NH_2NO[52]

$$H_2N-NO \rightleftharpoons HN-NOH \qquad (4)$$

In FTIR spectral bands were found, which could be attributed to nitrosamine-like species.[5,51] Our calculated energy was −217 kJ/mol. This step is accompanied by a change of the oxidation number. The N atom of the amino group is oxidized from −3 to −2 and the N atom of NO is reduced from +2 to +1. A large lowering of the energy to −383 kJ/mol arises in the next step (**5**), where a hydrogen atom bound to a nitrogen atom of the V−NH−NOH species is transferred to the OH group. The barrier for this step is 138 kJ/mol. This should be compared to 192 kJ/mol of a BLYP calculation of Kobayashi et al.[53] for the gas-phase reaction H_2N-NOH to HNN + H_2O. Our barrier is substantially lower because the V−N bond facilitates the migration of the hydrogen compared to the gas-phase reaction of the H_2N-NOH system. This step leads to a desorption of H_2O and N_2 and finally to a new formation of the V−O−V bridge (**6**). The relative energy for the latter intermediate is −295 kJ/mol. Although the desorption is endothermic, it proceeds irreversibly at low partial pressures. In the intermediates **4**−**6** the vanadyl group is reduced to the Brønsted acid V−OH. The spin density calculated with MSINDO is almost exclusively localized on the V atom of the reaction center. This can be interpreted as a transition from $V^{5+}(d^0)$ to $V^{4+}(d^1)$.

At the adjacent V═O group reaction steps analogous to **1** to **6** occur. Via the intermediates **7** to **12** the adjacent V═O group is similarly reduced to V−OH. The corresponding relative energies were E_{rel}(**7**) = −417 kJ/mol, E_{rel}(**8**) = −450 kJ/mol, E_{rel}(**9**) = −428 kJ/mol, E_{rel}(**10**) = −500 kJ/mol, E_{rel}(**11**) = −732 kJ/mol, and E_{rel}(**12**) = −595 kJ/mol. At the end of this chain two NO and two NH_3 were converted to two N_2 and two H_2O and the catalyst contains two V−OH groups connected by an oxygen atom. With electron paramagnetic resonance (EPR) spectroscopy signals were measured at $V_2O_5-WO_3/TiO_2$ catalysts, which can be attributed to antiferromagnetic d^1-d^1 ion pairs such as $V^{4+}-V^{4+}$.[54] For intermediate **12** singlet and triplet states were calculated with MSINDO and the triplet state with one unpaired electron at each V atom was found to be more stable by 129 kJ/mol. This situation is in line with the EPR experiments, but we did not take into account the antiferromagnetic coupling. Before a further reduction of the catalyst can be achieved, the catalyst must be reoxidized. This process starts with the adsorption of an O_2 molecule at one of the reduced V centers. As in intermediates **2** and **8** the V_2O_7 species is modified in such a way that an isolated reduced O_3V-OH species is generated and the other V center is tetrahedrally surrounded by the adsorbate, an OH group and two surface oxygen atoms (**13**). Both oxygen atoms of O_2 form bonds to the vanadium atom. This intermediate has an energy of −1107 kJ/mol. In the reaction step from **12** to **13** the system changes from the triplet to the singlet state.

In the following the adsorbed O_2 molecule abstracts a hydrogen atom from the OH group at the adjacent V center. A possible side reaction could be the dissociation of O_2 and the subsequent adsorption of one O atom at a Ti atom of the support. The hydrogen abstraction facilitates the approach of an NH_3 and leads to the formation of intermediate **14** (Figure 4). In the reaction step from **13** to **14** an O_3V-OH species is reoxidized to VO_4. The corresponding energy is −1029 kJ/mol. In the next step an NH_3 molecule is adsorbed at the reoxidized VO_4 species (**15**). The adsorption energy E_{rel}(**15**) − E_{rel}(**14**) is −89 kJ/mol, which is substantially smaller than the adsorption energy E_{rel}(**7**) − E_{rel}(**6**) with a value of −122 kJ/mol or the adsorption energy −128 kJ/mol for intermediate (**1**). This can be explained by the assumption that the VO_4 species is less reactive than the V_2O_7 species or the polymeric metavanadates.[55,56] This is reflected also in the shorter V−O bond lengths of the V−O−Ti bridges. In intermediate **16** the NH_3 molecule has transferred an H atom to the OH group of the (HO)V−O−OH species under formation of an H_2O molecule and an NH_2 group. The corresponding energy is −1177 kJ/mol. In **16** a vanadyl group V═O is formed at the second V center so that the catalyst is

reoxidized. In the following step (**17**) the tautomerized nitrosamine species V−NH−NOH is formed by reaction of an amine and an NO of the gas phase with a relative energy of −1144 kJ/mol. This means an energy loss of 33 kJ/mol compared to **16**. In **3** and **10** the formation of nitrosamine led to an energy gain of −91 and −73 kJ/mol, respectively. This can be explained by the localized spin density at the V center in **3** and **10**. In the doublet ground state of **17** the spin density is mainly localized on the O atom, which bridges the two V^{5+} ions. Such a situation is energetically less favorable.

The NH−NOH species is decomposed into H_2O and N_2 under formation of intermediate **18** with a relative energy of −1316 kJ/mol. The N_2 molecule is here still weakly bound to the V atom. After full desorption of N_2 intermediate **19** is formed with an energy of −1283 kJ/mol. Then the H atom of the OH group is transferred to the neighboring vanadyl oxygen resulting in intermediate **20** with an energy of −1283 kJ/mol.

In the next step an NH_3 molecule is bound to the vanadium of the VO_4 species **21** with a relative energy of −1360 kJ/mol. The adsorption energy with respect to **20** is therefore −77 kJ/mol. The absolute value is only 12 kJ/mol less than the −89 kJ/mol for the transition from **14** to **15**.

In intermediate **22** the NH_3 molecule has reacted with the OH group of the neighboring V center. In this process the V_2O_7 species is rearranged as in the intermediates **2**, **8**, and **13**. Here the energy is −1275 kJ/mol. Intermediate **23** is again a nitrosamine species, which has been formed by the reaction of the NH_2 group with NO. The energy is −1589 kJ/mol. The transition from **22** and **23** is therefore accompanied by an energy lowering of −314 kJ/mol. This is substantially more than for the comparable process from **2** to **3**, **9** to **10**, and **16** to **17**. The intermediate **22** is a doublet state. The spin density is here almost exclusively localized on the N atom. In contrast to the other nitrosamine formations the reaction product **23** is a closed shell system. The means that a spin pairing is reached in the reaction of V−NH_2 with NO, explaining the large energy gain. The nitrosamine is decomposed in the next step into N_2 and H_2O. Both reaction products are still weakly bound to the V center (**24**) accompained by a lowering of the energy to −1745 kJ/mol. In the final step N_2 and H_2O are desorbed and the catalyst is open for a new cycle.

In addition to the reaction intermediates a search for transition states with an optimization of the transition structures was performed for each reaction step. To keep the computer time at a feasible level, the second derivatives of the energy were numerically calculated from the analytical first derivatives only for those atoms involved in the reaction process. For the rest of the atoms a Davidon−Fletcher−Powell (DFP) algorithm was used. The transition structures are characterized by single negative roots of the Hesse matrix of the second derivatives. Figure 5 shows the energy profile along the reaction pathway. Table 3 lists the energy barriers for each step. The NH_3 adsorption for the steps **R** → **1**, **6** → **7**, **14** → **15**, and **20** → **21** occurred without any barrier. This is in accordance with temperature programmed desorption (TPD) experiments.[44−47] The highest barriers of 110−145 kJ/mol are connected with steps where the V_2O_7 species is strongly modified, i.e., for **1** → **2**, **5** → **6**, **7** → **8**, **11** → **12**, and **24** → **P**. They are larger than the activation energies deduced from SCR experiments which are in the range 46−54[21] or 59−63 kJ/mol.[57,58] However, our values are close to those obtained by Gilardoni et al.[11,59] by DFT calculations that are in the range of 113−146 kJ/mol. But these authors investigated a mechanism for NH_3 adsorbed at Brønsted acid sites of V_2O_5 without TiO_2. A reason for the discrepancy between our high calculated barriers and the lower experimental values could be that under experimental conditions the transition structures are stabilized by hydrogen bonding. Such stabilization effects have been observed in polar solvents.[52]

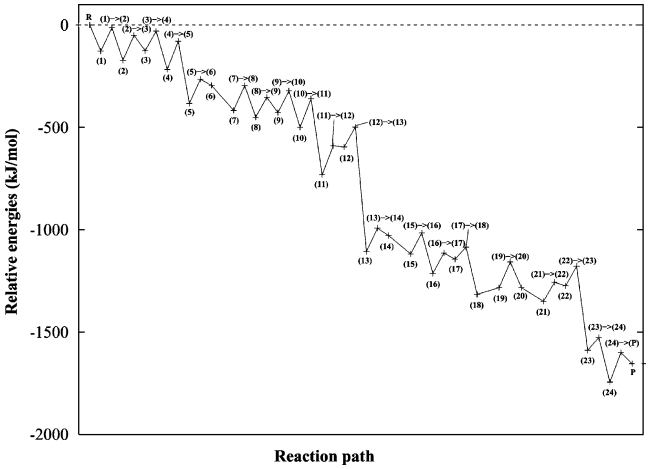

Figure 5. Energy profile (kJ/mol) for eq 1 along reaction pathway; bold numbers correspond to species in Table 1.

TABLE 3: Activation Barriers E_{act}[(I1) → (I2)] (kJ mol^{-1})

TS	M^b	E_{act}[(**I1**) → (**I2**)]	TS	M^b	E_{act}[(**I1**) → (**I2**)]
(**R**[a]) → (**1**)	1		(**13**) → (**14**)	1	114
(**1**) → (**2**)	1	115	(**14**) → (**15**)	1	
(**2**) → (**3**)	1	122	(**15**) → (**16**)	1	102
(**3**) → (**4**)	2	96	(**16**) → (**17**)	2	100
(**4**) → (**5**)	2	138	(**17**) → (**18**)	2	59
(**5**) → (**6**)	2	118	(**18**) → (**19**)	2	
(**6**) → (**7**)	2		(**19**) → (**20**)	2	125
(**7**) → (**8**)	2	121	(**20**) → (**21**)	2	
(**8**) → (**9**)	2	97	(**21**) → (**22**)	2	93
(**9**) → (**10**)	3	106	(**22**) → (**23**)	1	96
(**10**) → (**11**)	3	140	(**23**) → (**24**)	1	62
(**11**) → (**12**)	3	142	(**24**) → (**P**[a])	1	145
(**12**) → (**13**)	1	97			

[a] R: reactants. P: products. [b] *M*: multiplicity.

4. Conclusion

Semiempirical MSINDO calculations were sucessful in explaining the complicated reaction mechanism of NO reduction via NH_3 on a V_2O_5/TiO_2 surface. The anatase (100) surface structure is suitable for the deposition of VO_4 or polyvanadate-like species. Here the vanadium atom is only tetrahedrally coordinated and can be readily approached by the reactants. The full cycle involved 24 reaction steps with an equal number of intermediates and a corresponding number of transition structures. It could be shown that the reaction pathway is thermodynamically feasible due to the significant energy gain related to the formation of N_2. It was demonstrated how the NH_3 is adsorbed and that NO reacts with the adsorbed NH_3 from the gas phase. Also the role of O_2 in the reaction process was clarified. An important role of the vanadium catalyst is to facilitate the NH_3 dissociation and to reduce the barrier for the tautomerization of the nitrosamine-like species. The results are in line with models derived from experimental data but are much more detailed, because each single reaction step is elucidated.

Acknowledgment. This work was partially supported by INTAS. We thank Prof. C. Minot, Prof. O. B. Lapina, and Dr. V. Borovkov for their cooperation and regular exchange of information on the progress of their work. The figures were drawn with the program SCHAKAL.

References and Notes

(1) Hocking, M. B. *Modern Chemical Technology and Emission Control*; Springer: Berlin, 1985.

(2) Bretschneider, B.; Kurfürst, J. *Air Pollution Control Technology*; Elsevier: Amsterdam, 1987.

(3) Cheremisinoff, P. N. *Air Pollution Control and Design for Industry*; Dekker: New York, 1993.

(4) Janssen, F. J. In *Handbook of Heterogeneous Catalysis*; Ertl, G., Knözinger, H., Weitkamp, J., Eds.; VCH: Weinheim, Germany 1997; p 1633.

(5) Busca, G.; Lietti, L.; Ramis, G.; Berti, F. *Appl. Catal. B* **1998**, *18*, 1.

(6) Inomata, M.; Miyamoto, A.; Murakami, Y. *J. Catal.* **1980**, *62*, 140. Miyamoto, A.; Kobayashi, K.; Inomata, M.; Murakami, Y. *J. Phys. Chem.* **1982**, *86*, 2945.

(7) Bosch, H.; Janssen, F. J. J. G.; van den Kerkhof, F. M. G.; Oldenziel, J.; van Ommen, J. G.; Ross, J. R. H. *Appl. Catal.* **1986**, *25*, 239.

(8) Vogt, E. T. C.; van Dillen, A. J.; Geuss, J. W.; Janssen, F. J. J. G.; van den Kerkhof, F. M. G. *J. Catal.* **1989**, *119*, 269.

(9) Janssen, F.; van den Kerkhof, F.; Bosch, H.; Ross, J. *J. Phys. Chem.* **1987**, *91*, 5931.

(10) Janssen, F.; van den Kerkhof, F.; Bosch, H.; Ross, J. *J. Phys. Chem.* **1987**, *91*, 6633.

(11) Gilardoni, F.; Weber, J.; Baiker, A. *Int. J. Quantum Chem.* **1997**, *61*, 683.

(12) Zhanpeisov, N. U.; Higashimoto, S.; Anpo, M. *Int. J. Quantum Chem.* **2001**, *84*, 677.

(13) Anstrom, M.; Topsøe, N. Y.; Dumesic, J. A. *J. Catal.* **2003**, *213*, 115.

(14) Calatayud, M.; Mguig, B.; Minot, C. *Surf. Sci. Rep.*, submitted for publication.

(15) Lapina, O. B.; Shubin, A. A.; Nosov, A. V.; Bosch, E.; Spengel, J.; Knözinger, H. *J. Phys. Chem. B* **1999**, *103*, 7599.

(16) Zenkovets, G. A.; Kryukova, G. N.; Tsybulya, S. V.; Al'kaeva, E. M.; Andrushkevich, T. V.; Lapina, O. B.; Burgina, E. B.; Dovlitova, L. S.; Malakhov, V. V.; Litvak, G. S. *Kinet. Katal.* **2000**, *41*, 572.

(17) Deo, G.; Wachs, I. E. *J. Phys. Chem.* **1991**, *95*, 5889.

(18) Deo, G.; Wachs, I. E. *J. Catal.* **1994**, *146*, 335.

(19) Forzatti, P. *Appl. Catal. A* **2001**, *222*, 221.

(20) Bulushev, D. A.; Kiwi-Minsker, L.; Rainone, F.; Renken, A. *J. Catal.* **2002**, *205*, 115.

(21) Lietti, L.; Forzatti, P. *J. Catal.* **1994**, *147*, 241.

(22) Pinaeva, L. G.; Lapina, O. B.; Mastikhin, V. M.; Nosov, A. V.; Balzhimaev, B. S. *J. Mol. Catal.* **1994**, *88*, 311.

(23) Bond, G. C. *Catal. Today* **1994**, *20*, 125.

(24) Bond, G. C.; Tahir, S. I. *Appl. Catal.* **1991**, *71*, 1.

(25) Cristiani, C.; Forzatti, P.; Busca, G. *J. Catal.* **1990**, *124*, 586.

(26) Ramis, G.; Cristiani, C.; Forzatti, P.; Busca, G. *J. Catal.* **1990**, *124*, 574.

(27) Eckert, H.; Wachs, I. E. *J. Phys. Chem.* **1989**, *93*, 6796.

(28) Larrubia, M. A.; Busca, G. *Mater. Chem. Phys.* **2001**, *72*, 337.

(29) Busca, G. *J. Raman Spectrosc.* **2002**, *33*, 348.

(30) Sayle, D. C.; Catlow, C. R. A.; Perrin, M. A.; Nortier, P. *J. Phys. Chem.* **1996**, *100*, 8940.

(31) Calatayud, M.; Mguig, B.; Minot, C. *Surf. Sci.* **2003**, *526*, 297.

(32) Kachurovskaya, N. A.; Zhidomirov, G. M.; Minot, C. *Surf. Rev. Lett.* **2002**, *9*, 1425.

(33) Kachurovskaya, N. A.; Mikheeva, E. P.; Zhidomirov, G. M. *J. Mol. Catal. A* **2002**, *178*, 191.

(34) Bredow, T.; Jug, K. *J. Phys. Chem.* **1995**, *99*, 285.

(35) Zhanpeisov, N. V.; Bredow, T.; Jug, K. *Catal. Lett.* **1996**, *39*, 111.

(36) Nanda, D. N.; Jug, K. *Theor. Chim. Acta* **1980**, *57*, 95.

(37) Li, J.; Correa de Mello, P.; Jug, K. *J. Comput. Chem.* **1992**, *13*, 85.

(38) Ahlswede, B.; Jug, K. *J. Comput. Chem.* **1999**, 563.

(39) Ahlswede, B.; Jug, K. *J. Comput. Chem.* **1999**, 572.

(40) Bredow, T.; Geudtner, G.; Jug, K. *J. Comput. Chem.* **2001**, *22*, 861.

(41) Homann, T.; Bredow, T.; Jug, K. *Surf. Sci.* **2002**, *515*, 205.

(42) Homann, T.; Bredow, T.; Jug, K. *Surface Sci.*, in press.

(43) Bredow, T.; Homann, T.; Jug, K. *Res. Chem. Int.*, in press.

(44) Koebel, M.; Elsener, M. *Chem. Eng. Sci.* **1998**, *53*, 657.

(45) Efstatio, A. M.; Fliatoura, K. *Appl. Catal. B* **1995**, *6*, 35.

(46) Srnak, T. Z.; Dumesic, J. A.; Clausen, B. S.; Tornqvist, E.; Topsøe, N. Y. *J. Catal.* **1992**, *135*, 246.

(47) Tronconi, E.; Lietti, L.; Forzatti, P.; Malloggi, S. *Chem. Eng. Sci.* **1996**, *51*, 2965.

(48) Inomata, M.; Miyamoto, A.; Murakami, Y. *J. Catal.* **1980**, *62*, 140.

(49) Nova, I.; Lietti, L.; Tronconi, E.; Forzatti, P. *Catal. Today* **2000**, *60*, 73.

(50) Dumesic, J. A.; Topsøe, N. Y.; Topsøe, H.; Chen. Y.; Slabiak, T. *J. Catal.* **1996**, *163*, 409.

(51) Ramis, G.; Busca, G.; Bregani, F.; Forzatti, P. *Appl. Catal.* **1990**, *64*, 259.

(52) Hollemann, A. F.; Wiberg, E. *Lehrbuch der Anorganischen Chemie*, 101st ed.; Walter de Gruyter: Berlin, New York 1995.

(53) Kobayashi, Y.; Tajima, N.; Hirao, K. *J. Phys. Chem. A* **2000**, *104*, 6855.

(54) Védrine, J. C. *Catal. Today* **2000**, *56*, 455.

(55) Alemany, J. L.; Lietti, L.; Ferlazzo, N.; Forzatti, P.; Busca, G.; Ramis, G.; Giamello, E.; Bregani, F. *J. Catal.* **1995**, *155*, 117.

(56) Went, G. T.; Leu, L. J.; Bell, J. *J. Catal.* **1992**, *134*, 479.

(57) Lietti, L.; Nova, I.; Camurri, S.; Tronconi, E.; Forzatti, P. *AIChE J.* **1997**, *43*, 2559.

(58) Marshneva, V. I.; Slavinskaya, E. M.; Kalinkina, O. V.; Odegova, G. V.; Moroz, E. M.; Lavrova, G. V.; Salanov, A. N. *J. Catal.* **1995**, *155*, 171.

(59) Gilardoni, F.; Weber, J.; Baiker, A. *J. Phys. Chem. A* **1997**, *101*, 6069.